

PALEOECOLOGY

Cryogenian evolution of stigmasteroid biosynthesis

Yosuke Hoshino,^{1*} Aleksandra Poshibaeva,² William Meredith,³ Colin Snape,³ Vladimir Poshibaev,² Gerard J. M. Versteegh,^{4,5} Nikolay Kuznetsov,^{2,6} Arne Leider,¹ Lennart van Maldegem,^{1,4} Mareike Neumann,¹ Sebastian Naehrer,^{1,4†} Małgorzata Moczyłowska,⁷ Jochen J. Brocks,⁸ Amber J. M. Jarrett,⁸ Qing Tang,⁹ Shuhai Xiao,⁹ David McKirdy,¹⁰ Supriyo Kumar Das,¹¹ José Javier Alvaro,¹² Pierre Sansjofre,¹³ Christian Hallmann^{1,4‡}

Sedimentary hydrocarbon remnants of eukaryotic C₂₆–C₃₀ sterols can be used to reconstruct early algal evolution. Enhanced C₂₉ sterol abundances provide algal cell membranes a density advantage in large temperature fluctuations. Here, we combined a literature review with new analyses to generate a comprehensive inventory of unambiguously syngenetic steranes in Neoproterozoic rocks. Our results show that the capacity for C₂₉ 24-ethyl-sterol biosynthesis emerged in the Cryogenian, that is, between 720 and 635 million years ago during the Neoproterozoic Snowball Earth glaciations, which were an evolutionary stimulant, not a bottleneck. This biochemical innovation heralded the rise of green algae to global dominance of marine ecosystems and highlights the environmental drivers for the evolution of sterol biosynthesis. The Cryogenian emergence of C₂₉ sterol biosynthesis places a benchmark for verifying older sterane signatures and sets a new framework for our understanding of early algal evolution.

INTRODUCTION

All modern eukaryotes biosynthesize sterols or acquire them through dietary uptake. Incorporated into the cell membrane, they are essential for homeostasis and cell signaling within this domain (1), and their concentration in lipid rafts plays a significant role for budding and endocytosis through affecting membrane curvature (2). Given the rarity of extended sterol biosynthesis in bacteria (3), steranes preserved in sediments and ancient rocks have been frequently used as fossil biomarkers diagnostic of ancient eukaryotes. The large diversity of sterols in living cells is principally defined by double bonds and functional moieties that show limited survival after cell death (4). Diagenetic processes during sedimentary burial largely reduce the structural diversity of residual steroids to variations in their (C-24) side-chain alkylation, leaving mostly three major saturated sterane hydrocarbons containing 27, 28, or 29 carbon atoms: cholestane, ergostane, and stigmastane. Hence, it is predominantly this tripartite diversity that allows for paleobiogeochemical reconstructions of past eukaryotic diversity.

The geological record of steranes

Systematic changes in the relative abundance of these three steranes have been observed over the course of the past ~550 million years of Earth history. A continuously increasing relative abundance of ergostanes (5), for example, has been attributed to the global rise and radiation of chlorophyll *c*-containing phytoplankton (6). Significantly less is known about the initial rise and early evolution of the eukaryote lineage. Molecular clocks place the last eukaryotic common ancestor at ~1.8 billion years ago (7), whereas the oldest unambiguously eukaryotic acritarch microfossils date to ca. 1.6 billion years ago (8). However, this consensus date had been distorted for more than one decade by false biomarker positives: Sedimentary steranes in Proterozoic rocks [for example, (9)] and up to 2.7 billion years in age (10) steered discussions of a much earlier eukaryotic dawning. Only the advent of enhanced contamination awareness (11, 12) and an unprecedented clean drilling operation (13) persuasively unmasked Archean steranes as modern contaminants. As a positive corollary, the burden of proof for the detection of indigenous and syngenetic sterane biomarkers throughout the Precambrian was significantly raised and led us to systematically (re-)analyze both previously studied and new Proterozoic sedimentary sequences with an unexpected outcome. We here report on the heterogeneous diversity and palaeogeographic distribution of unambiguously indigenous (Supplementary Materials) steranes throughout the Neoproterozoic, a finding that changes our understanding of early eukaryotic steroid biosynthesis and evolution.

The composite molecular inventory of Phanerozoic rocks, petroleum, or modern environmental samples virtually always contains the C_{27–29} steroid troika in varying relative abundances (1, 4, 5). In broad terms, cholesterol biosynthesis is dominant in metazoa and rhodophyceae, whereas elevated abundances of C₂₉ phytosterols are biosynthesized by green algae and higher plants. However, it is noteworthy that even pure cultures of eukaryotic algae only rarely display an exclusive steroidal end-member dominance (4, 5, 14). It is only the early rock record that deviates significantly from this balanced pattern: A C₂₇-only steroidal distribution in the Tonian Chuar Group (15) was recently reconfirmed and supplemented by two other similarly aged deposits, which appear devoid of any conventional C₂₈ or C₂₉ steranes (16). On the other

Copyright © 2017
The Authors, some
rights reserved;
exclusive licensee
American Association
for the Advancement
of Science. No claim to
original U.S. Government
Works. Distributed
under a Creative
Commons Attribution
NonCommercial
License 4.0 (CC BY-NC).

¹Max Planck Institute for Biogeochemistry, Hans-Knoell-Strasse 10, 07745 Jena, Germany. ²Gubkin Russian State University of Oil and Gas, Leninsky Prospekt 65, Moscow, Russia. ³Faculty of Engineering, University of Nottingham, Energy Technologies Building, Triumph Road, Nottingham NG7 2TU, UK. ⁴MARUM—Center for Marine Environmental Sciences, University of Bremen, Leobener Strasse 8, 28359 Bremen, Germany. ⁵Alfred Wegener Institut, Helmholtz-Zentrum für Polar- und Meeresforschung, Am Handelshafen 12, 27570 Bremerhaven, Germany. ⁶Geological Institute, Russian Academy of Sciences, Pygeevsky 7, Moscow, Russia. ⁷Department of Earth Sciences, Uppsala University, Villavägen 16, 752 36 Uppsala, Sweden. ⁸Research School of Earth Sciences, Australian National University, Building 142, Mills Road, Canberra, Australian Capital Territory 2601, Australia. ⁹Department of Geosciences, Virginia Tech, Blacksburg, VA 24061, USA. ¹⁰Department of Earth Science, The University of Adelaide, Adelaide, South Australia 5005, Australia. ¹¹Department of Geology, Presidency University, College Street 86/1, Kolkata 700073, India. ¹²Instituto de Geociencias (Consejo Superior de Investigaciones Científicas—Universidad Complutense de Madrid), Novais 12, 28040 Madrid, Spain. ¹³Laboratoire Géosciences Océan, UMR CNRS-6538, Université de Bretagne Occidentale, 29280 Plouzane, France.

*Present address: School of Biological Sciences, Georgia Institute of Technology, 950 Atlantic Drive Northwest, Atlanta, GA 30332, USA.

†Present address: GNS Science, 1 Fairway Drive, Avalon, Lower Hutt 5010, New Zealand.

‡Corresponding author. Email: chhallmann@bgc-jena.mpg.de

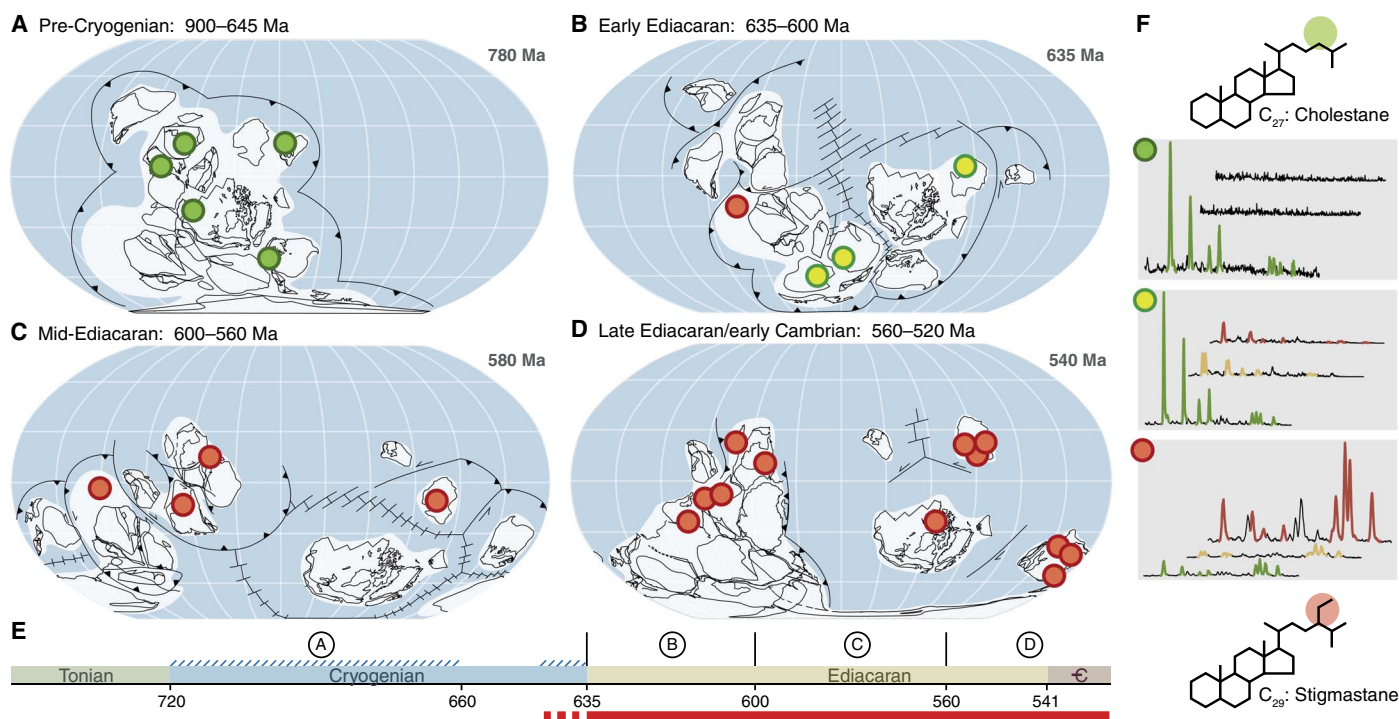


Fig. 1. Evolutionary radiation of stigmasteroid (24) biosynthesis. (A) Tonian rocks are nearly exclusively characterized by C₂₇ steranes [cholestane; see (F): Green symbols denote C₂₇ dominance and complete absence of C₂₉ steranes, with only sporadic traces of C₂₈ 4-desmethylsteranes]. (B) The oldest noncontaminated C₂₉ 24-ethylsteranes [stigmastane; see (F): yellow symbols stand for C₂₇ > C₂₉, whereas red symbols indicate C₂₇ < C₂₉ and often C₂₇ ≪ C₂₉] only appear during the latest Cryogenian (Marinoan deglaciation) and earliest Ediacaran in Oman, whereas contemporaneous rocks from three other localities are still strongly or exclusively dominated by C₂₇ steranes, indicating a 720- to 635-Ma Snowball Earth glacial origin of the stigmasteroid biosynthetic pathway—in agreement with the physiological membrane density advantage yielded by cellular phytosterols (19, 20) and molecular clocks (30). (C and D) Global dominance of C₂₉ steroid biosynthesis by 600 Ma (table S1) highlights the evolutionary advantage of the likely chlorophyte host organism and a rapid rise to ecological dominance. (E) Schematic representation of Neoproterozoic time showing steroidal dominance (green, C₂₇ versus red, C₂₉) and the time brackets from (A) to (D). (F) Relevant molecular structures and schematic tandem-MS chromatograms of (bottom to top) C₂₇ [green, mass/charge ratio (*m/z*) 372 to 217], C₂₈ (yellow, *m/z* 386 to 217), and C₂₉ (red, *m/z* 400 to 217) steranes, emphasizing the color code used in (A) to (D). Ages on the top right of the maps comply with the palaeogeographic snapshots after (31).

end of the C₂₇–₂₉ steroidal spectrum, it has long been known that certain Ediacaran to Early Cambrian oils in Oman, Siberia, and India are strongly dominated by C₂₉ steranes (6). However, because of the migrated nature of these petroleum fluids and the large temporal data gap spanning the Ediacaran, virtually nothing has been known on the timing and distribution of rising C₂₉ steroid abundances or what this peculiar signal could mean.

RESULTS AND DISCUSSION

With additional analyses and a literature survey, we now convincingly show that the Late Ediacaran dominance of C₂₉ steranes does not represent rare or isolated depositional environments. This signature is not restricted merely to particular lithologies, latitudes, or facies zones (table S1), but instead seems representative of a highly uniform global steroid metabolism during the Late Ediacaran (Fig. 1), as confirmed by 67 samples from 14 localities (Supplementary Materials). Despite the rarity of thermally well-preserved and organic rich sedimentary strata of pre-Cryogenian age, we find that also in this time slice [ca. 900 to 720 million years ago (Ma)], the predominance of C₂₇ steranes is not dependent on environmental factors (table S1) but appears inherent to global steroid metabolism before the Cryogenian, whereas common C₂₉ steranes are systematically absent in all 35 samples from five localities spanning the globe (Fig. 1).

Steroid biosynthesis and physiology

Across all clades—including some bacteria—steroid biosynthesis starts with the epoxidation of squalene (17), followed by enzymatic cyclization to one of two possible C₃₀ protosterols: lanosterol or cycloartenol (1, 4). Although the evolutionary relationship between the lanosterol and cycloartenol cyclases has recently been found to be more complex than previously assumed (3), downstream modifications of lanosterol to both C₂₇ and C₂₈ sterols conserve the same reaction order of demethylations (C-4 and C-14) performed by the same enzymes after methylation at C-24 (4), but do not lead to 24-ethyl (C₂₉) steroids. Cycloartenol, on the contrary, can be a precursor to C₂₇–C₂₉ sterols (18) following a different reaction order, thus pointing to a separate evolutionary origin of this pathway and implying that cycloartenol biosynthesis likely preceded the emergence of C₂₉ sterols. This provides a plausible explanation for the sporadic co-occurrence of C₂₈ ergostane traces alongside the pre-Cryogenian C₂₇ signal (table S1), whereas C₂₉ steranes are systematically absent. A high compositional diversity of lipids is thought to ensure a stable and impermeable membrane even when cellular composition, osmolarity, or pH is changed because of physiological or pathological events (2, 4). The presence of C₂₉ sterols in “raft-like” model membranes significantly lessens temperature dependence of membrane dynamics, as compared to systems with C₂₇ and C₂₈ sterols, suggesting that C₂₉ 24-ethylsterols are produced to extend the temperature range in which membrane-associated

biological processes can take place (19). Hence, the use of C_{29} sterols yields an important advantage to large temperature fluctuations, and it has been hypothesized that this adaptive “membrane tuning” represents an evolutionary response to large temperature variations (20).

The Neoproterozoic Snowball Earth events—two severe glacial episodes within the time interval 717 to 632 Ma (21, 22), whose globally distributed diamictite remnants reflect the magnitude and spatial extent of these glaciations (23)—represent the most pervasive climatic perturbation in all of Earth’s history. However, the biological consequences, in particular whether Neoproterozoic life experienced an evolutionary bottleneck or a catalyst, are unclear. C_{29} 24-ethylsteranes (24) are systematically absent from sediments deposited before the onset of the Snowball Earth events (Fig. 1A) but are present in rocks deposited during and directly after the Marinoan deglaciation (Fig. 1B), implying an origin of stigmasteroid (24) biosynthesis during the glaciation. Whereas subglacial water temperatures during the Cryogenian glaciations were relatively constant as a result of vigorous convective mixing (25), large diurnal temperature variations would have existed in low-latitude cryoconite pans (26). Recent climate models imply ice-free tropical continents (27), whose wind-blown dust would have created ablated glacial surfaces with meltwater above low-albedo accumulations of dust, biomass, and degraded organic matter (28). The modern equivalents of these cryoconite holes host diverse bacterial and eukaryotic communities and can be considered individual ecosystems (29). Hence, small and isolated eukaryotic populations were exposed to strong environmental forcing by frequent large temperature variations (27) in habitats with limited or periodic population mixing—providing an ideal scenario for beneficial mutation and localized evolutionary selection toward more successful C_{29} -sterol producing algae.

The ecological rise of green algae

The localized evolution of stigmasteroid (24) biosynthesis is suggested by a postglacial gradient: Around 635 Ma, that is, during and directly after the Marinoan deglaciation, eukaryotes in the South Oman Salt Basin (SOSB) were already dominated by C_{29} sterol-producing species, whereas the algal community in three other coeval locations still largely consisted of eukaryotes synthesizing C_{27} sterols (Fig. 1B). A C_{29} sterane dominance in carbonates and shales that are embedded within the Marinoan diamictite in the SOSB—thus possibly up to 645 Ma in age (Supplementary Materials)—firmly places the rise of this biosynthetic capacity within, and not directly after, the Cryogenian. Although C_{29} sterol-synthesizing algae are dominant in only one locality between 635 and 600 Ma, they had reached global dominance at the latest by 600 to 560 Ma (Fig. 1C). This rapid global radiation testifies to the exceptional ecological success of stigmasteroid-producing algae and, in turn, suggests that this biosynthetic capacity must have emerged during the Cryogenian glaciations and not earlier. Green algae predominantly biosynthesize C_{29} sterols (1, 4–6, 14), dominate modern cryoconites (29), and likely existed before the Cryogenian (7). With molecular clocks indicating a Late Cryogenian divergence of green algal SMT genes (*carbon-24/28-sterol methyltransferase* responsible for C-24 methylation of sterols) from those of other Archaeplastida (fig. S1) (30), our data suggest that stigmasteroid biosynthesis emerged in an ancestral green alga and subsequently led to the rise of this group to ecological dominance.

CONCLUSIONS

Dating the evolving sterol biosynthetic pathway not only provides a unique and precise calibration point for molecular clock studies of

biochemical processes but also places a new benchmark for reliably recognizing steroid contamination in pre-Cryogenian sediments. Considering biochemical innovation and the physiological function of membrane lipids within a well-dated geological framework brings us closer to understanding the environmental drivers of evolving organismic complexity and sets a new framework for our understanding of early eukaryotic evolution.

MATERIALS AND METHODS

For this study, we summarized selected biomarker data from the literature, where the indigeneity of components was evident or highly likely (see the Supplementary Materials for approach and rationale), and performed laboratory analyses on sedimentary rock samples. We analyzed the molecular inventory of 158 Neoproterozoic rocks, of which 61 yielded trustworthy and reliable steroidal signatures that were deemed as unambiguously syngenetic (table S1, Supplementary Materials). Five studied formations did not yield a single sample with uncontaminated steroidal signatures (table S2). Furthermore, 68 selectively chosen Neoproterozoic sterane values from the literature were used (table S1).

Rock sample preparation and workup

Samples were analyzed using standard organic geochemical techniques under measures of extreme precaution, similar to techniques that we previously reported (13, 32). In brief, samples were first separated into interior and exterior portions, either by sawing using a diamond-rimmed blade-fitted stainless steel saw [Lortone; blade cleaned by ultrasound-assisted solvent extraction in dichloromethane (DCM) and by baking at 450°C for 8 hours] or by the microablation technique (33). Sample interiors and exteriors were separately crushed and ground to a fine powder using a shatterbox (Siebtechnik, Scheibenschwingmühle) fitted with a custom-made stainless steel puck and mill, which were cleaned by baking at 500°C for 8 hours. In between samples, the puck and mill were cleaned by grinding and discarding clean quartz sand five times and by solvent rinsing with DCM. The resulting sample powders were solvent-extracted (DCM) by ultrasound agitation in Teflon vessels or by using a CEM Mars 6 microwave extraction approach (up to 30 g of powder extracted with three times 30 ml of DCM under stirring at 120°C for 20 min each). The resulting total lipid extracts were desulfurized using activated (with HCl_{aq}), neutralized, and solvent-extracted copper pellets and fractionated on silica gel columns into saturated hydrocarbons (SAT), aromatic hydrocarbons, and polar compounds, as described in more detail elsewhere (32). SAT were spiked with internal standards ($C_{30}D_{62}$ triacontane and d_4 -5 α -cholestane) and analyzed using coupled gas chromatography (GC) and mass spectrometry (MS).

GC and MS

Full-scan analyses were performed on a Trace GC Ultra (Thermo Scientific) coupled to an ALMSCO BenchTOF-dx mass spectrometer. The gas chromatograph was fitted with a VF-1 MS column [40 m; inner diameter (i.d.), 0.15 mm; film thickness, 0.15 μ m] and operated with a constant flow (1.4 ml/min) of helium (99.999% pure, Westfalen AG) as a carrier gas. Samples (between 1 out of 50 and 1 out of 500 μ l) were injected in splitless mode using a programmed temperature vaporizer injector (ramped from 60° to 315°C at 14.5°/s). The GC oven was held at 60°C (2 min) before ramping at 4.5°/min to a final temperature of 325°C, which was held for 10 min. Ionization was

achieved at 70 eV (electron impact) and 250°C with a filament current of ca. 4 A. Data were measured from m/z 30 to 800 but only recorded from m/z 50 to 550 at ca. 1000 mass resolution using 2469 scans per scanset and a scanset period of 250 ms. Analytes were quantified by comparison to internal standards without correcting for individual response factors.

Target compound analysis for biomarkers (including steranes) was performed on a Thermo Quantum XLS Ultra triple-quadrupole mass spectrometer coupled to a Thermo Trace GC Ultra, fitted with a DB-XLB capillary column (60 m; i.d., 0.25 mm; film thickness, 0.25 μm) and a deactivated precolumn (10 m; i.d., 0.53 mm). A constant flow (1.3 ml/min) of helium (99.999 % pure, Westfalen AG) was used as a carrier gas. Volumes of typically 1 or 2 μl out of 50 to 200 μl were injected on column at 70°C. The oven was held isothermal at 70°C (5 min), then heated to 335°C at 4°/min, and held at the final temperature for 9 min. Ionization was achieved by electron impact at 70 eV and 250°C, with an emission current of 50 μA . Q1 and Q3 were each operated in 0.7-Da resolution with a cycle time of 0.5 s. Q2 was operated with Argon 5.0 collision gas at a pressure of 1.1 mtorr and varying collision voltages depending on the target analyte. Compounds were quantified on characteristic parent-to-daughter ion mass transitions (for C_{27} – C_{29} steranes: m/z 372, 386, and 400 fragmenting to m/z 217) relative to d_4 -5 α -cholestane (m/z 376 fragmenting to m/z 221) without correcting for differential response factors.

Hydropyrolysis of kerogens

For hydropyrolysis (University of Nottingham), aliquots of 60 to 125 mg of purified kerogen were mixed with ammonium dioxodithiomolybdate catalyst. First, a procedural blank was run and tested negative (GC-MS at the University of Nottingham) for steranes. Subsequently, each sample/catalyst mixture was interspersed with ~100 mg of pre-extracted and calcined acid-washed quartz sand to “bulk out” the sample and prevent reactor blockage. A thermal desorption step was run from ambient to 250°C at 300°/min and subsequently to 350°C at 8°/min and held for 2 min, during which released “free” hydrocarbons were trapped on silica. After changing the trap silica, a pyrolysis step was run from ambient to 350°C at 300°C/min, then to 520°C at 8°/min, and held for 2 min, during which covalently bound hydrocarbons were “cracked” and trapped on silica. Between samples, the system was cleaned thoroughly: Reactor tubes and fittings were cleaned by ultrasound-assisted extraction in DCM, followed by heating to 550°C (30 min) in the HyPy system.

Identification of SMT genes

Genes coding for two SMT enzymes in the green alga *Ostreococcus lucimarinus* were identified from the literature (30) and via GenBank (www.ncbi.nlm.nih.gov/). A homologous sequence search in green algae was carried out in GenBank using BLASTp with a cutoff threshold of $<1 \times 10^{-5}$.

SUPPLEMENTARY MATERIALS

Supplementary material for this article is available at <http://advances.sciencemag.org/cgi/content/full/3/9/e1700887/DC1>

Supplementary Text

fig. S1. Molecular clock analysis of SMT genes (30) reveals a divergence of green algae during the Late Cryogenian.

fig. S2. Studied sample locations on a modern continental configuration.

fig. S3. Studied sample locations in a palaeogeographic context after (31).

fig. S4. Estimated maximum time brackets of the studied samples.

fig. S5. Hydropyrolysis of an earliest Ediacaran cap carbonate sample from the Mirassol d'Oeste Fm verifies the C_{27} sterane-dominated signature found in other samples from this unit and confirms their syngenicity to the host rock.

table S1. Steranes in Neoproterozoic rocks.

table S2. Unsuitable samples.

References (34–122)

REFERENCES AND NOTES

1. J. K. Volkman, Sterols and other triterpenoids: Source specificity and evolution of biosynthetic pathways. *Org. Geochem.* **36**, 139–159 (2005).
2. K. Simons, J. L. Sampaio, Membrane organization and lipid rafts. *Cold Spring Harb. Perspect. Biol.* **3**, a004697 (2011).
3. J. H. Wei, X. Yin, P. Welander, Sterol synthesis in diverse bacteria. *Front. Microbiol.* **7**, 990 (2016).
4. R. E. Summons, A. S. Bradley, L. L. Jahnke, J. R. Waldbauer, Steroids, triterpenoids and molecular oxygen. *Philos. Trans. R. Soc. B* **361**, 951–968 (2006).
5. P. J. Grantham, L. L. Wakefield, Variations in the sterane carbon number distributions of marine source rock derived crude oils through geological time. *Org. Geochem.* **12**, 61–73 (1988).
6. A. H. Knoll, R. E. Summons, J. W. Waldbauer, J. E. Zumberge, The geological succession of primary producers in the oceans, in *Evolution of Primary Producers in the Sea*, P. Falkowski, A. H. Knoll, Eds. (Elsevier, 2007), pp. 133–163.
7. L. W. Parfrey, D. J. G. Lahr, A. H. Knoll, L. A. Katz, Estimating the timing of early eukaryotic diversification with multigene molecular clocks. *Proc. Natl. Acad. Sci. U.S.A.* **108**, 13624–13629 (2011).
8. K. Pang, Q. Tang, J. D. Schiffbauer, J. Yao, X. Yuan, B. Wan, L. Chen, Z. Ou, S. Xiao, The nature and origin of nucleus-like intracellular inclusions in Paleoproterozoic eukaryote microfossils. *Geobiology* **11**, 499–510 (2013).
9. A. Dutkiewicz, S. C. George, D. J. Mossman, J. Ridley, H. Volk, Oil and its biomarkers associated with the Palaeoproterozoic Oklo natural fission reactors, Gabon. *Chem. Geol.* **244**, 130–154 (2007).
10. J. J. Brocks, G. A. Logan, R. Buick, R. E. Summons, Archean molecular fossils and the early rise of eukaryotes. *Science* **285**, 1033–1036 (1999).
11. J. J. Brocks, E. Grosjean, G. A. Logan, Assessing biomarker syngeneity using branched alkanes with quaternary carbon (BAQCs) and other plastic contaminants. *Geochim. Cosmochim. Acta* **72**, 871–888 (2008).
12. A. Leider, T. C. Schumacher, C. Hallmann, Enhanced procedural blank control for organic geochemical studies of critical sample material. *Geobiology* **14**, 469–482 (2016).
13. K. L. French, C. Hallmann, J. M. Hope, P. L. Schoon, J. Alex Zumberge, Y. Hoshino, C. A. Peters, S. C. George, G. D. Love, J. J. Brocks, R. Buick, R. E. Summons, Reappraisal of hydrocarbon biomarkers in Archean rocks. *Proc. Natl. Acad. Sci. U.S.A.* **112**, 5915–5920 (2015).
14. R. B. Kodner, A. Pearson, R. E. Summons, A. H. Knoll, Sterols in red and green algae: Quantification, phylogeny, and relevance for the interpretation of geologic steranes. *Geobiology* **6**, 411–420 (2008).
15. R. E. Summons, S. C. Brassell, G. Eglinton, E. Evans, R. J. Horodyski, N. Robinson, D. M. Ward, Distinctive hydrocarbon biomarkers from fossiliferous sediment of the late Proterozoic Walcott Member, Chuar Group, Grand-Canyon, Arizona. *Geochim. Cosmochim. Acta* **52**, 2625–2637 (1988).
16. J. J. Brocks, A. J. Jarrett, E. Sirantoine, F. Kenig, M. Moczyłowska, S. Porter, J. Hope, Early sponges and toxic protists: Possible sources of cryostane, an age diagnostic biomarker antedating Sturtian Snowball Earth. *Geobiology* **14**, 129–149 (2015).
17. T. T. Tchen, K. Bloch, On the mechanism of enzymatic cyclization of squalene. *J. Biol. Chem.* **226**, 931–939 (1957).
18. M. B. Miller, B. A. Haubrich, Q. Wang, W. J. Snell, W. D. Nes, Evolutionarily conserved $\Delta^{25(27)}$ -olefin ergosterol biosynthesis pathway in the alga *Chlamydomonas reinhardtii*. *J. Lipid Res.* **53**, 1636–1645 (2012).
19. J. G. Beck, D. Mathieu, C. Loudet, S. Buchoux, E. J. Dufourc, Plant sterols in ‘rafts’: A better way to regulate membrane thermal shocks. *FASEB J.* **21**, 1714–1723 (2007).
20. E. J. Dufourc, The role of phytosterols in plant adaptation to temperature. *Plant Signal. Behav.* **3**, 133–134 (2008).
21. A. D. Rooney, J. V. Strauss, A. D. Brandon, F. A. Macdonald, A Cryogenian chronology: Two long-lasting synchronous Neoproterozoic glaciations. *Geology* **43**, 459–462 (2015).
22. A. R. Prave, D. J. Condon, K. H. Hoffmann, S. Tapster, A. E. Fallick, Duration and nature of the end-Cryogenian (Marinoan) glaciation. *Geology* **44**, 631–634 (2016).
23. P. F. Hoffman, D. P. Schrag, The snowball Earth hypothesis: Testing the limits of global change. *Terra Nova* **14**, 129–155 (2002).
24. Referring to all C_{29} 4-desmethyl-24-ethyl-sterols, which are converted to stigmastane (C_{29} 24-ethyl-cholestane) after diagenesis.

25. Y. Ashkenazy, H. Gildor, M. Losch, F. A. Macdonald, D. P. Schrag, E. Tziperman, Dynamics of a Snowball Earth ocean. *Nature* **495**, 90–93 (2013).
26. P. Hoffman, Cryoconite pans on Snowball Earth: Supraglacial oases for Cryogenian eukaryotes? *Geobiology* **14**, 531–542 (2016).
27. D. I. Benn, G. Le Hir, H. Bao, Y. Donnadieu, C. Dumas, E. J. Fleming, M. J. Hambrey, E. A. McMillan, M. S. Petronis, G. Ramstein, C. T. E. Stevenson, P. M. Wynn, I. J. Fairchild, Orbitally forced ice sheet fluctuations during the Marinoan Snowball Earth glaciation. *Nat. Geosci.* **8**, 704–708 (2015).
28. R. A. Wharton Jr., C. P. McKay, G. M. Simmons Jr., B. C. Parker, Cryoconite holes on glaciers. *BioScience* **35**, 499–503 (1985).
29. J. Uetake, T. Naganuma, M. B. Hebsgaard, H. Kanda, S. Kohshima, Communities of algae and cyanobacteria on glaciers in west Greenland. *Polar Sci.* **4**, 71–80 (2010).
30. D. A. Gold, J. Grabenstatter, A. de Mendoza, A. Riesgo, I. Ruiz-Trillo, R. E. Summons, Sterol and genomic analyses validate the sponge biomarker hypothesis. *Proc. Natl. Acad. Sci. U.S.A.* **113**, 2684–2689 (2016).
31. Z.-X. Li, D. A. D. Evans, G. P. Halverson, Neoproterozoic glaciations in a revised global palaeogeography from the breakup of Rodinia to the assembly of Gondwanaland. *Sediment. Geol.* **294**, 219–232 (2013).
32. C. Hallmann, A. E. Kelly, S. N. Gupta, R. E. Summons, Reconstructing deep-time biology with molecular fossils, in *Quantifying the Evolution of Early Life: Numerical Approaches to the Evaluation of Fossils and Ancient Ecosystems*, M. Laflamme, J. D. Schiffbauer, S. Q. Dornbos, Eds. (Springer, 2011) vol. 36, pp. 355–401.
33. A. J. M. Jarrett, R. Schintee, J. M. Hope, J. J. Brocks, Micro-ablation, a new technique to remove drilling fluids and other contaminants from fragmented and fissile rock material. *Org. Geochem.* **61**, 57–65 (2013).
34. E. Grosjean, G. A. Logan, Incorporation of organic contaminants into geochemical and an assessment of potential sources: Examples from Geoscience Australia marine survey S282. *Org. Geochem.* **38**, 853–869 (2007).
35. C. J. Illing, C. Hallmann, K. E. Miller, R. E. Summons, H. Strauss, Airborne contamination from laboratory atmospheres. *Org. Geochem.* **76**, 26–38 (2014).
36. Y. Hoshino, S. C. George, Cyanobacterial inhabitation on Archean rock surfaces in the Pilbara Craton, Western Australia. *Astrobiology* **15**, 559–574 (2015).
37. J. J. Brocks, Millimeter-scale concentration gradients of hydrocarbons in Archean shales: Live-oil escape or fingerprint of contamination? *Geochim. Cosmochim. Acta* **75**, 3196–3213 (2011).
38. S. C. Brassel, J. McEvoy, C. F. Hoffmann, N. A. Lamb, J. R. Maxwell, Isomerisation, rearrangement and aromatisation of steroids in distinguishing early stages of diagenesis. *Org. Geochem.* **6**, 11–23 (1984).
39. T. M. Peakman, J. R. Maxwell, Early diagenetic pathways of steroid alkenes. *Org. Geochem.* **13**, 583–592 (1988).
40. A. S. Mackenzie, R. L. Patience, J. R. Maxwell, M. Vandenbroucke, B. Durand, Molecular parameters of maturation in the Toarcian shales, Paris Basin, France—I. Changes in the configurations of acyclic isoprenoid alkanes, steranes and triterpanes. *Geochim. Cosmochim. Acta* **44**, 1709–1721 (1980).
41. K. E. Peters, J. M. Moldowan, *The Biomarker Guide* (Prentice Hall, 1993).
42. A. S. Mackenzie, Application of biological markers in petroleum geochemistry, in *Advances in Petroleum Geochemistry*, Vol. 1, J. Brooks, D. H. Welte, Eds. (Academic Press, 1984), pp. 115–214.
43. J. A. Curiale, Origin of solid bitumens, with emphasis on biological marker results. *Org. Geochem.* **10**, 559–580 (1986).
44. H. Mißbach, J.-P. Duda, N. K. Lünsdorf, B. C. Schmidt, V. Thiel, Testing the preservation of biomarkers during experimental maturation of an immature kerogen. *Int. J. Astrobiol.* **15**, 165–175 (2016).
45. L. Dong, S. Xiao, B. Shen, X. Yuan, X. Yan, Y. Peng, Restudy of the worm-like carbonaceous compression fossils *Protoarenicola*, *Pararenicola*, and *Sinosabellidites* from early Neoproterozoic successions in North China. *Palaeogeogr. Palaeoclimatol. Palaeoecol.* **258**, 138–161 (2008).
46. Q. Tang, K. Pang, X. Yuan, S. Xiao, Electron microscopy reveals evidence for simple multicellularity in the Proterozoic fossil *Chuarina*. *Geology* **45**, 75–78 (2017).
47. C. Yin, Micropaleoflora from the Late Precambrian in Huainan region of Anhui Province and its stratigraphic significance, in *Professional Papers of Stratigraphy and Paleontology* (Chinese Academy of Geological Sciences, 1985), vol. 12, pp. 97–119.
48. Q. Tang, K. Pang, S. Xiao, X. Yuan, Z. Ou, B. Wan, Organic-walled microfossils from the early Neoproterozoic Liulaoabei Formation in the Huainan region of North China and their biostratigraphic significance. *Precambrian Res.* **236**, 157–181 (2013).
49. M. K. Stevens, S. N. Apak, GSWA Empress 1 and 1A well completion report, Yowalga Sub-basin, Officer Basin, Western Australia (Geological Survey of Western Australia, Record 1999/4, 1999).
50. N. J. Butterfield, The Neoproterozoic. *Curr. Biol.* **25**, R859–R836 (2015).
51. A. C. Hill, K. L. Cotter, K. Grey, Mid-Neoproterozoic biostratigraphy and isotope stratigraphy in Australia. *Precambrian Res.* **100**, 281–298 (2000).
52. N. L. Swanson-Hysell, A. C. Maloof, J. L. Kirschvink, D. A. D. Evans, G. P. Halverson, M. T. Hurtgen, Constraints on Neoproterozoic paleogeography and Paleozoic orogenesis from paleomagnetic records of the Bitter Springs Formation, Amadeus Basin, central Australia. *Am. J. Sci.* **312**, 817–884 (2012).
53. A. J. M. Jarrett, Biogeochemical evolution in the Neoproterozoic Amadeus Basin, central Australia, doctoral thesis, The Australian National University (2015).
54. K. E. Karlstrom, S. A. Bowring, C. M. Dehler, A. H. Knoll, S. M. Porter, D. J. Des Marais, A. B. Weil, Z. D. Sharp, J. W. Geissman, M. B. Elrick, J. M. Timmons, L. J. Crossey, K. L. Davidek, Chuar Group of the Grand Canyon: Record of breakup of Rodinia, associated change in the global carbon cycle, and ecosystem expansion by 740 Ma. *Geology* **28**, 619–622 (2000).
55. S. A. Bowring, J. P. Grotzinger, D. J. Condon, J. Ramezani, M. J. Newell, P. A. Allen, Geochronologic constraints on the chronostratigraphic framework of the Neoproterozoic Huqf Supergroup, Sultanate of Oman. *Am. J. Sci.* **307**, 1097–1145 (2007).
56. M. Modczyłowska, V. Pease, S. Willman, L. Wickström, H. Agić, A Tonian age for the Visingsö Group in Sweden constrained by detrital zircon dating and biochronology: Implications for evolutionary events, *Geological Magazine In Press* (Cambridge Univ. Press, 2017).
57. G. Vidal, Late Precambrian microfossils from the basal sandstone unit of the Visingsö beds, South Sweden. *Geol. Palaeontol.* **8**, 1–14 (1974).
58. G. Vidal, *Acritarchs and the Correlation of the Upper Proterozoic* (Publications from the Institutes of Mineralogy, Paleontology and Quaternary Geology, University of Lund, 1979), vol. 219.
59. M. Marti Mus, M. Modczyłowska, Internal morphology and taphonomic history of the Neoproterozoic vase-shaped microfossils from the Visingsö Group, Sweden. *Nor. Geol. Tidsskr.* **80**, 213–228 (2000).
60. P. Sansjofre, R. I. F. Trindade, M. Ader, J. L. Soares, A. C. R. Nogueira, N. Tribouillard, Paleoenvironmental reconstruction of the Ediacaran Araras platform (Western Brazil) from the sedimentary and trace metals record. *Precambrian Res.* **241**, 185–202 (2014).
61. A. C. R. Nogueira, C. Riccomini, A. N. Sial, C. A. V. Moura, R. I. F. Trindade, T. R. Fairchild, Carbon and strontium isotope fluctuations and paleoceanographic changes in the late Neoproterozoic Araras carbonate platform, southern Amazon craton, Brazil. *Chem. Geol.* **237**, 168–190 (2007).
62. M. Babinski, R. I. F. Trindade, C. J. S. Alvarenga, P. C. Boggiani, D. Liu, R. V. Santos, B. B. Brito Neves, Chronology of Neoproterozoic ice ages in Central Brazil, in *First Symposium on Neoproterozoic-Early Paleozoic Events in SW Gondwana. Extended Abstracts. IGCP Project 478* (Sao Paulo, Brazil, 2004), pp. 303–306.
63. M. Deynoux, P. Affaton, R. Trompette, M. Villeneuve, Pan-African tectonic evolution and glacial events registered in Neoproterozoic to Cambrian cratonic and foreland basins of West Africa. *J. Afr. Earth Sci.* **46**, 397–426 (2006).
64. M. Villeneuve, Review of the orogenic belts on the western side of the West African craton: The Bassarides, Rokelides and Mauritanides, in *The Boundaries of the West African Craton*, N. Ennih, J. P. Liégeois, Eds. (Geological Society of London Special Publication 2008), vol. 297, pp. 169–202.
65. D. Lahondère, J. Roger, J. Le Metour, M. Donzeau, F. Guillocheau, C. Helm, D. Thieblemont, A. Cocherie, C. Guerrot, Notice explicative des cartes géologiques à 1/200 000 et 1/500 000 de l'extrême Sud de la Mauritanie (DMG, Min. Mines Ind., Nouakchott, Rap. BRGM/RC-54273-FR, 2005).
66. J. J. Álvaro, M. Macouin, B. Bauluz, S. Clausen, M. Ader, The Ediacaran sedimentary architecture and carbonate productivity in the Atar cliffs, Adrar, Mauritania: Palaeoenvironments, chemostratigraphy and diagenesis. *Precambrian Res.* **153**, 236–261 (2007).
67. G. A. Shields, M. Deynoux, H. Strauss, H. Paquet, D. Nahon, Barite-bearing cap dolostones of the Taoudéni basin, northwest Africa: Sedimentary and isotopic evidence for methane seepage after a Neoproterozoic glaciation. *Precambrian Res.* **153**, 209–235 (2007).
68. G. A. Shields, M. Deynoux, S. J. Culver, M. D. Braiser, P. Affaton, D. Vandamme, Neoproterozoic glaciomarine and cap dolostone facies of the southwestern Taoudéni Basin (Walidiala Valley, Senegal/Guinea, NW Africa). *C. R. Geosci.* **339**, 186–199 (2007).
69. G. A. Shields-Zhou, M. Deynoux, L. Och, The record of Neoproterozoic glaciation in the Taoudéni Basin, NW Africa, in *The Geological Record of Neoproterozoic Glaciations*, E. Arnaud, G. P. Halverson, G. A. Shields-Zhou, Eds. (Geological Society of London Memoirs, 2011), vol. 36, pp. 163–171.
70. J. K. Sovetov, Late Cryogenian (Vendian) glaciogenic deposits in the Marnya Formation, Oselok Group, in the foothills of the East Sayan Range, southwestern Siberian Craton, in *The Geological Record of Neoproterozoic Glaciations*, E. Arnaud, G. P. Halverson, G. A. Shields-Zhou, Eds. (Geological Society of London Memoirs, 2011), vol. 36, pp. 317–329.
71. J. K. Sovetov, Tillites at the base of the Vendian Taseeva Group in the stratotype section (Siberian craton). *Russ. Geol. Geophys.* **56**, 1522–1530 (2015).

72. B. G. Pokrovsky, M. I. Bujakaite, O. V. Kokin, Geochemistry of C, O and Sr isotopes and chemostratigraphy of Neoproterozoic rocks in the Northern Yenisei Ridge. *Lith. Min. Resour.* **47**, 177–199 (2012).
73. G. P. Halverson, G. Shields-Zhou, Chemostratigraphy and the Neoproterozoic glaciations, in *The Geological Record of Neoproterozoic Glaciations*, E. Arnaud, G. P. Halverson, G. A. Shields-Zhou, Eds. (Geological Society of London Memoirs, 2011), vol. 36, pp. 51–66.
74. V. G. Kuznetsov, Riphean hydrocarbon reservoirs of the Yurubchen-Tokhom zone, Lena-Tunguska province, NE Russia. *J. Pet. Geol.* **20**, 459–474 (1997).
75. E. Grosjean, G. D. Love, C. Stalvies, D. A. Fike, R. E. Summons, Origin of petroleum in the Neoproterozoic-Cambrian South Oman Salt Basin. *Org. Geochem.* **40**, 87–110 (2009).
76. P. F. Hoffman, A. J. Kaufman, G. P. Halverson, D. P. Schrag, A neoproterozoic snowball Earth. *Science* **281**, 1342–1346 (1998).
77. D. A. Fike, J. P. Grotzinger, L. M. Pratt, R. E. Summons, Oxidation of the Ediacaran ocean. *Nature* **444**, 744–747 (2006).
78. F. A. Macdonald, M. D. Schmitz, J. L. Crowley, C. F. Roots, D. S. Jones, A. C. Maloof, J. V. Strauss, P. A. Cohen, D. T. Johnston, D. P. Schrag, Calibrating the Cryogenian. *Science* **327**, 1241–1243 (2010).
79. P. M. Myrow, A. J. Kaufman, A newly discovered cap carbonate above Varanger-age glacial deposits in Newfoundland, Canada. *J. Sediment. Res.* **69**, 784–793 (1999).
80. S. A. Pisarevski, P. J. A. McCausland, J. P. Hodych, S. J. O'Brien, J. A. Tait, J. B. Murphy, Paleomagnetic study of the late Neoproterozoic Bull Arm and Crown Hill formations (Musgravetown Group) of eastern Newfoundland: Implications for Avalonia and West Gondwana paleogeography. *Can. J. Earth Sci.* **49**, 308–327 (2012).
81. J. P. Pu, S. A. Bowring, J. Ramezani, P. Myrow, T. D. Raub, E. Landing, A. Mills, E. Hodgkin, F. A. Macdonald, Dodging snowballs: Geochronology of the Gaskiers glaciation and the first appearance of the Ediacaran biota. *Geology* **44**, 955–958 (2016).
82. M. Osburn, J. Grotzinger, G. Love, K. D. Bergmann, A. Sessions, Deposition and diagenesis of the Ediacaran Khufai Formation, Huqf Supergroup, Oman: Preservation potential for the Shuram carbon isotopic excursion, paper presented at the AAPG Annual Conference and Exhibition, Houston, Texas, 10 to 13 April 2011.
83. G. D. Love, E. Grosjean, C. Stalvies, D. A. Fike, J. P. Grotzinger, A. S. Bradley, A. E. Kelly, M. Bhatia, W. Meredith, C. E. Snape, S. A. Bowring, D. J. Condon, R. E. Summons, Fossil steroids record the appearance of Demospongiae during the Cryogenian period. *Nature* **457**, 718–721 (2009).
84. G. Jiang, N. Christie-Blick, A. J. Kaufman, D. M. Banerjee, V. Rai, Sequence stratigraphy of the Neoproterozoic Infra Krol Formation and Krol Group, Lesser Himalaya, India. *J. Sediment. Res.* **72**, 524–542 (2002).
85. A. J. Kaufman, G. Jiang, N. Christie-Blick, D. M. Banerjee, V. Rai, Stable isotope record of the terminal Neoproterozoic Krol platform in the lesser Himalayas of northern India. *Precambrian Res.* **147**, 156–185 (2006).
86. K. Grey, M. R. Walter, C. R. Calver, Neoproterozoic biotic diversification: Snowball Earth or aftermath of the Acraman impact? *Geology* **31**, 459–462 (2003).
87. W. V. Preiss, The Adelaide Geosyncline of South Australia and its significance in Neoproterozoic continental reconstructions. *Precambrian Res.* **100**, 21–63 (2000).
88. J. P. Grotzinger, D. A. Fike, W. W. Fischer, Enigmatic origin of the largest-known carbon isotope excursion in Earth's history. *Nat. Geosci.* **4**, 285–292 (2011).
89. C. R. Calver, J. F. Lindsay, Ediacaran sequence and isotope stratigraphy of the Officer Basin, South Australia. *Aust. J. Earth Sci.* **45**, 513–532 (1998).
90. D. M. McKirdy, L. J. Webster, K. R. Arouri, K. Grey, V. A. Gostin, Contrasting sterane signatures in Neoproterozoic marine rocks of Australia before and after the Acraman asteroid impact. *Org. Geochem.* **37**, 189–207 (2006).
91. D. Condon, M. Zhu, S. Bowring, W. Wang, A. Yang, Y. Jin, U-Pb ages from the Neoproterozoic Doushantuo Formation, China. *Science* **308**, 95–98 (2005).
92. J. Craig, J. Thurow, B. Thusu, A. Whitham, Y. Abutarruma, Global Neoproterozoic petroleum systems: The emerging potential in North Africa, in *Global Neoproterozoic Petroleum Systems: The Emerging Potential in North Africa*, J. Craig, J. Thurow, B. Thusu, A. Whitham, Y. Abutarruma, Eds. (Geological Society of London Special Publication, 2009), vol. 326, pp. 1–25.
93. W. Ahmad, S. Alam, Organic geochemistry and source rock characteristics of Salt Range Formation, Potwar Basin, Pakistan. *Pak. J. Hydrocarb. Res.* **17**, 37–59 (2007).
94. J. Craig, U. B. Numbers, R. F. Galimberti, K. A. R. Ghori, J. D. Gortner, N. Hakho, D. P. Le Heron, J. Thurow, M. Vecoli, The paleobiology and geochemistry of Precambrian hydrocarbon source rocks. *Mar. Petrol. Geol.* **40**, 1–47 (2013).
95. J. Ram, Neoproterozoic successions in peninsular India and their hydrocarbon prospectivity, in *Geology and Hydrocarbon Potential of Neoproterozoic–Cambrian Basins in Asia*, G. M. Bhat, J. Craig, J. W. Thurow, B. Thusu, A. Cozzi, Eds. (Geological Society of London Special Publication, 2012), vol. 366, pp. 59–73.
96. K. E. Peters, M. E. Clark, V. Dasgupta, M. A. McCaffrey, C. Y. Lee, Recognition of an Infracambrian source rock based on biomarkers in the Bhagewala-1. Oil India. *AAPG Bull.* **79**, 1482–1494 (1995).
97. S. Dutta, S. Bhattacharya, S. V. Raju, Biomarker signatures from Neoproterozoic–Early Cambrian oil, western India. *Org. Geochem.* **56**, 68–80 (2013).
98. A. Cozzi, G. Rea, J. Craig, From global geology to hydrocarbon exploration: Ediacaran–Early Cambrian petroleum plays of India, Pakistan and Oman, in *Geology and Hydrocarbon Potential of Neoproterozoic–Cambrian Basins in Asia*, G. M. Bhat, J. Craig, J. W. Thurow, B. Thusu, A. Cozzi, Eds. (Geological Society of London Special Publication, 2012), vol. 366, pp. 131–162.
99. O. K. Bazhenova, O. A. Arefiev, Geochemical peculiarities of Pre-Cambrian source rocks in the East European platform. *Org. Geochem.* **25**, 341–351 (1996).
100. M. A. Fedonkin, P. Vickers-Rich, The White Sea's windswept coast, in *The Rise of Animals: Evolution and Diversification of the Kingdom Animalia*, M. A. Fedonkin, J. G. Gehling, K. Grey, G. M. Narbonne, P. Vickers-Rich, Eds. (Johns Hopkins Univ. Press, 2007), pp. 115–146.
101. M. Moczydlowska, F. Westall, F. Foucher, Microstructure and biogeochemistry of the organically preserved Ediacaran Metazoan *Sabellidites*. *J. Paleol.* **88**, 224–239 (2014).
102. S. A. Bowring, J. P. Grotzinger, C. E. Isachsen, A. H. Knoll, S. M. Pelechaty, P. Kolosov, Calibrating rates of early Cambrian evolution. *Science* **261**, 1293–1298 (1993).
103. D. V. Grazhdankin, U. Balthasar, K. E. Nagovitsin, B. B. Kochnev, Carbonate-hosted Ediacaran-type fossils in arctic Siberia. *Geology* **36**, 803–806 (2008).
104. F. M. Gradstein, J. Ogg, A. Phanerozoic time scale. *Episodes* **19**, 3–6 (1996).
105. J. P. Duda, V. Thiel, J. Reitner, D. Grazhdankin, Opening up a window into ecosystems with Ediacara-type organisms: Preservation of molecular fossils in the Khatyspyt Lagerstätte (Arctic Siberia). *PalZ* **90**, 659–671 (2016).
106. B. Shen, S. Xiao, L. Dong, C. Zhou, J. Liu, Problematic macrofossils from Ediacaran successions in the North China and Chaidam blocks: Implications for their evolutionary roots and biostratigraphic significance. *J. Paleol.* **81**, 1396–1411 (2007).
107. M. Zhu, J. Zhang, A. Yang, G. Li, M. Steiner, B. D. Erdtmann, Sinian-Cambrian stratigraphic framework for shallow- to deep-water environments of the Yangtze Platform: An integrated approach. *Prog. Nat. Sci.* **13**, 951–960 (2003).
108. M. Zhu, J. Zhang, A. Yang, Integrated Ediacaran (Sinian) chronostratigraphy of South China. *Palaeogeogr. Palaeoclimatol. Palaeoecol.* **254**, 7–61 (2007).
109. J. E. Amthor, J. P. Grotzinger, S. Schröder, S. A. Bowring, J. Ramezani, M. W. Martin, A. Matter, Extinction of Cloudina and Namacalathus at the Precambrian-Cambrian boundary in Oman. *Geology* **31**, 431–434 (2003).
110. J. Dahl, J. M. Moldowan, R. E. Summons, L. A. McCaffrey, P. Lipton, D. S. Watt, J. M. Hope, Extended β -alkyl steranes and 3-alkyl triaromatic steroids in crude oils and rock extracts. *Geochim. Cosmochim. Acta* **59**, 3717–3729 (1995).
111. A. A. Petrov, S. D. Pustil'nikova, N. N. Abriutina, G. R. Kagramonova, Petroleum steranes and triterpanes. *Neftekhimiya* **16**, 411–427 (1976).
112. W. K. Seifert, J. M. Moldowan, E. J. Gallegos, Application of mass spectrometry to petroleum exploration, in *Mass Spectrometric Characterization of Shale Oils*, T. Aczel, Ed. (ASTM Special Technical Publication 902, 1986), pp. 121–147.
113. M. G. Fowler, A. G. Douglas, Saturated hydrocarbon biomarkers in oils of Late Precambrian age from Eastern Siberia. *Org. Geochem.* **11**, 201–213 (1987).
114. R. E. Summons, T. G. Powell, Hydrocarbon composition of the Late Proterozoic oils of the Siberian Platform: Implications for the depositional environment of source rocks, in *Early Organic Evolution: Implications for Mineral and Energy Resources*, M. Schidlowski, S. Golubic, M. Kimberley, D. McKirdy, P. A. Trudinger, Eds. (Springer, 1992), pp. 296–307.
115. T. A. Jones, C. W. Jefferson, G. R. Morrell, Assessment of mineral and energy resource potential in the Brock Inlier–Bluenose Lake area, N.W.T. (Geological Survey of Canada Open File 2434, 1992).
116. J. B. W. Wielens, H. von der Dick, M. G. Fowler, P. W. Brooks, F. Monnier, Geochemical comparison of a Cambrian algalite potential source rock, and hydrocarbons from the Colville/Tweed lake area, Northwest territories. *Bull. Can. Pet. Geol.* **38**, 236–245 (1990).
117. M. F. Fowler, The influence of *Gloeocapsamorpha prisca* on the organic geochemistry of oils and organic-rich rocks of Late Ordovician age from Canada, in *Early Organic Evolution: Implications for Mineral and Energy Resources*, M. Schidlowski, S. Golubic, M. Kimberley, D. McKirdy, P. A. Trudinger, Eds. (Springer, 1992), pp. 336–358.
118. M. R. Rezaee, X. Sun, Fracture-filling cements in the Palaeozoic Warburton Basin, South Australia. *J. Pet. Geol.* **30**, 79–90 (2007).
119. J. R. Laurie, Pre-Ordovician source rocks in Australia: A compilation, in *Proceedings of the Central Australian Basins Symposium III*, Alice Springs, NT, 16 to 17 July 2012.
120. C. O. E. Hallmann, K. R. Arouri, D. M. McKirdy, L. Schwark, A new perspective on exploring the Cooper/Eromanga/ petroleum province—Evidence of oil charging from the Warburton Basin. *APPEA J.* **46**, 261–282 (2006).
121. G. R. Sousa Júnior, A. C. R. Nogueira, E. V. Santos Neto, C. A. V. Moura, B. Q. Araújo, F. de A. M. Reis, Organic matter in the Neoproterozoic cap carbonate from the Amazonian Craton, Brazil. *J. South Am. Earth Sci.* **72**, 7–24 (2016).
122. M. Elie, A. C. R. Nogueira, A. Nédélec, R. I. F. Trindade, F. Kenig, A red algal bloom in the aftermath of the Marinoan Snowball Earth. *Terra Nova* **19**, 303–308 (2007).

Acknowledgments: We thank B. Nettersheim for the discussions and P. Pringle for the laboratory support. R. Summons is thanked for providing two samples. **Funding:** This study was principally funded by the Max Planck Society (Max Planck Research Group grant to C.H.); S.N. was supported by the Deutsche Forschungsgemeinschaft (Na1172/2-1). D.M. was supported by the Petroleum Branch of the Department of Primary Industries and Resources, South Australia. **Author contributions:** C.H. conceived and directed the study; Y.H., A.P., W.M., C.S., V.P., G.J.M.V., N.K., A.L., L.v.M., M.N., S.N., M.M., J.J.B., A.J.M.J., Q.T., S.X., D.M., S.K.D., J.J.A., and P.S. performed experiments and provided materials and data; Y.H. and C.H. analyzed the data; and C.H. and Y.H. wrote the paper with input from all the other authors. The contribution of D.M. to this paper comprises TRaX Record 384. **Competing interests:** The authors declare that they have no competing interests. **Data and materials availability:** All data needed to evaluate the conclusions in the paper are present in the paper and/or the

Supplementary Materials. Additional and raw data, as well as used sample material, related to this paper may be requested from the authors.

Submitted 22 March 2017

Accepted 30 August 2017

Published 20 September 2017

10.1126/sciadv.1700887

Citation: Y. Hoshino, A. Poshibaeva, W. Meredith, C. Snape, V. Poshibaev, G. J. M. Versteegh, N. Kuznetsov, A. Leider, L. van Maldegem, M. Neumann, S. Naeher, M. Moczyłowska, J. J. Brocks, A. J. M. Jarrett, Q. Tang, S. Xiao, D. McKirdy, S. K. Das, J. J. Alvaro, P. Sansjofre, C. Hallmann, Cryogenian evolution of stigmasteroid biosynthesis. *Sci. Adv.* **3**, e1700887 (2017).